Liu *et al. Heritage Science* (2024) 12:305
https://doi.org/10.1186/s40494-024-01415-x

Heritage Science

RESEARCH

Open Access

Study on the control effectiveness of relative humidity by various ventilation systems for the conservation of cultural relics

Benli Liu[1], Chenchen He[1,2], Guobin Zhang[3*], Ruihong Xu[3], Hongtao Zhan[3], Fasi Wu[3] and Dongpeng He[3]

Abstract

The Dadiwan F901 site, boasting a history of over 5000 years, stands as the largest and most intricately crafted large-scale housing structure from China's prehistoric era. The early renovation efforts, incorporating a sealed glass curtain wall, led to a continuous rise in relative humidity within the site, triggering outbreaks of microbial diseases. Subsequent measures successfully restored stability to the thermal and humid environment. This paper employs on-site real-time environmental monitoring and numerical simulation methods to assess the ventilation effectiveness and relative humidity changes before and after multiple interior modifications of the Dadiwan F901 site museum. The results indicate that the fully enclosed glass curtain wall can suppress the dependence of indoor humidity fluctuations on external weather fluctuations but has generated unintended consequences, leading to increased air relative humidity and even reaching saturation in the museum space. The strategic deployment of louvered windows and duct fans proved effective in enhancing internal airflow dynamics and overall air exchange capacity. It was possible to ensure that the relative humidity inside the site remained at approximately 70%, meeting the essential requirements for the preservation of cultural relics. This study is of great significance for alleviating the deterioration problem of enclosed exhibition halls of earthen relics.

Keywords Cultural relics preservation, Dadiwan F901, Relative humidity, Numerical simulation, Ventilation systems

*Correspondence:
Guobin Zhang
zhanggb@dha.ac.cn
Full list of author information is available at the end of the article

Graphical Abstract

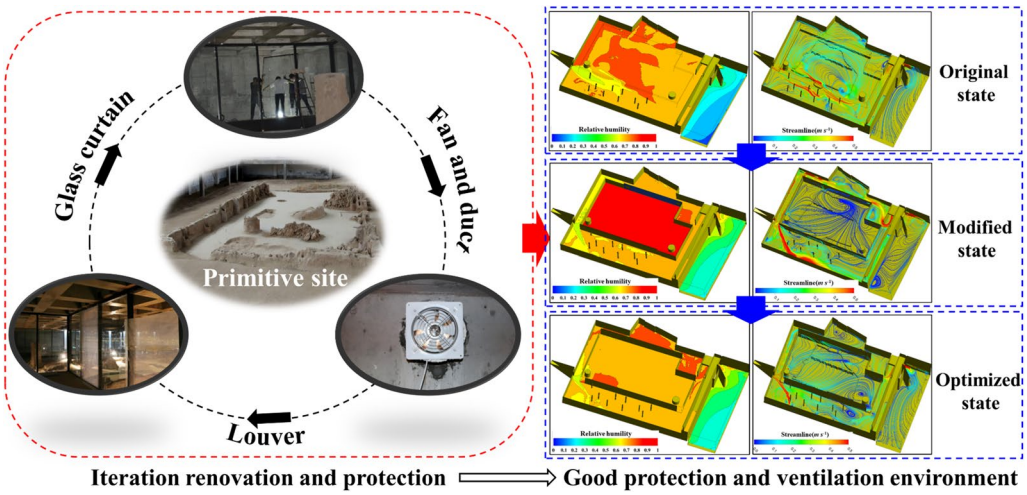

Introduction

The Dadiwan site is located in Qin'an County, Gansu Province, northwest China. It is known for its abundant cultural artifacts and unique characteristics, which reflect the ancient civilization established by the Chinese ancestors in the Yellow River Basin [1]. The site is considered one of the most important Neolithic sites in northwest China [2]. Its F901 site is the most prominent palace-style construction with a total area of 420 m^2, the largest and most highly crafted large-scale housing structure from China's prehistoric era [3, 4]. The origin of this structure may be traced back to the late phase of the Yangshao culture, approximately 5000 years ago [5, 6]. Its grand scale, intricate structure, and meticulous design pioneered the development of ceremonial palace-style architecture in China [7]. The museum on the site was finished in late 2011 and made accessible to the public. Its purpose is to accurately replicate the natural state of the ancient community, showcasing the activities, lifestyle, and ecological surroundings of early people. To avoid any direct human intervention, the museum effectively isolated the spot by constructing glass curtain walls. Nevertheless, this action resulted in a persistent increase in indoor temperatures and consistent saturation of relative humidity, which in turn caused the occurrence and spread of microbial diseases. As a result, this cultural relic experienced ongoing degradation caused by microbial diseases.

Excavation and conservation of artifacts disturb the previously steady subsurface environment, making the relics very vulnerable to harm [8]. Common forms of damage include deformation, cracking, efflorescence, blistering, separation of paint layers, discoloration, and microbiological diseases, among other manifestations [9–12]. The main environmental elements that contribute to the destruction of artifacts include temperature, relative humidity, and microbes [13]. Temperature variations may cause direct harm to artifacts by affecting materials with differing reaction rates, whereas changes in relative humidity can modify the moisture content of artifacts, resulting in structural and characteristic alterations [14]. The collective impact of these elements facilitates detrimental chemical reactions and the rapid growth of microorganisms, leading to the deterioration of artifacts [15]. In addition, the process of moisture evaporation may result in the movement of soluble salts from the soil to the surface, which can induce local crystallization, efflorescence, and the occurrence of whitening phenomena [14, 16]. Therefore, hygrothermal cycling plays an essential role in the development of deterioration [17].

Good ventilation can help control temperature, relative humidity, and air quality, thus slowing down the damage to cultural relics or sites. Natural ventilation is one of the most basic ventilation methods, achieved through the design and layout of the building to facilitate natural convection. Heating, ventilation, and air conditioning (HVAC) systems stand as the primary means to meet thermal and humidity requirements [18–21]. The heating system is often employed to enhance the climate stability of the museum [22]. Meanwhile, the air curtain system isolates the exhibition halls from the external environment to control the stability of the internal localized

environment [23, 24]. Compared to complex HVAC systems, displacement ventilation is widely used for local environmental control [8]. Environmentally sensitive artifacts or sites are usually isolated in sealed showcases to minimize the impact of the external environment [25, 26]. To minimize damage to the F901 site, the research staff have combined the above treatments and restorations to improve the airflow circulation and maintain the internal humidity-heat balance in the museum.

This research utilizes on-site real-time environmental monitoring and numerical simulation techniques to evaluate the airflow and relative humidity conditions of the Dadiwan F901 palace-style building site museum before and after many alterations. Firstly, an analysis is conducted on the variations in interior and outdoor temperature and relative humidity throughout various phases of protection. Secondly, a three-dimensional numerical simulation is created to accurately replicate the fluctuations of the environmental elements and evaluate the effectiveness of various protective measures. The model's accuracy is confirmed by comparison with observed data. This study not only provides a scientific basis for the development and implementation of protection protocols related to ventilation and air management in the Dadiwan site museum but also offers valuable insights and guidance for the preservation of similar cultural relics.

Methods

Study area

The Dadiwan F901 site is situated in the Wuying Township of Qin'an County, Gansu Province, Northwestern China (105.90°E, 35.01°N), positioned on the second and third terraces along with adjacent gentle slope mountainous terrain on the southern bank of the Qingshui River, a tributary of the Hulu River [27]. The site is located within the typical topographical features of the Loess Plateau. The region exhibits a semi-humid climate, characterized by an average annual temperature of 9.2℃ and an annual precipitation range of 507–561 mm. The geographic particulars are illustrated in Fig. 1.

In June 2018, the management authorities began renovating the Dadiwan F901 site. The chronological sequence of protective measures implemented for the site was condensed into several phases: Phase I (before June 2018, Fig. 2a), there were no precautions taken to guard against any potential harm, and the interior humidity levels fluctuated in accordance with the outdoor humidity. During phase II (Fig. 2b), which took place from June to October 2018, the installation of closed glass curtain walls was carried out on the site.

During phase III (Fig. 2c), which took place from October 2018 to May 2019, mechanical equipment such as louvered ventilation windows, and duct fans were

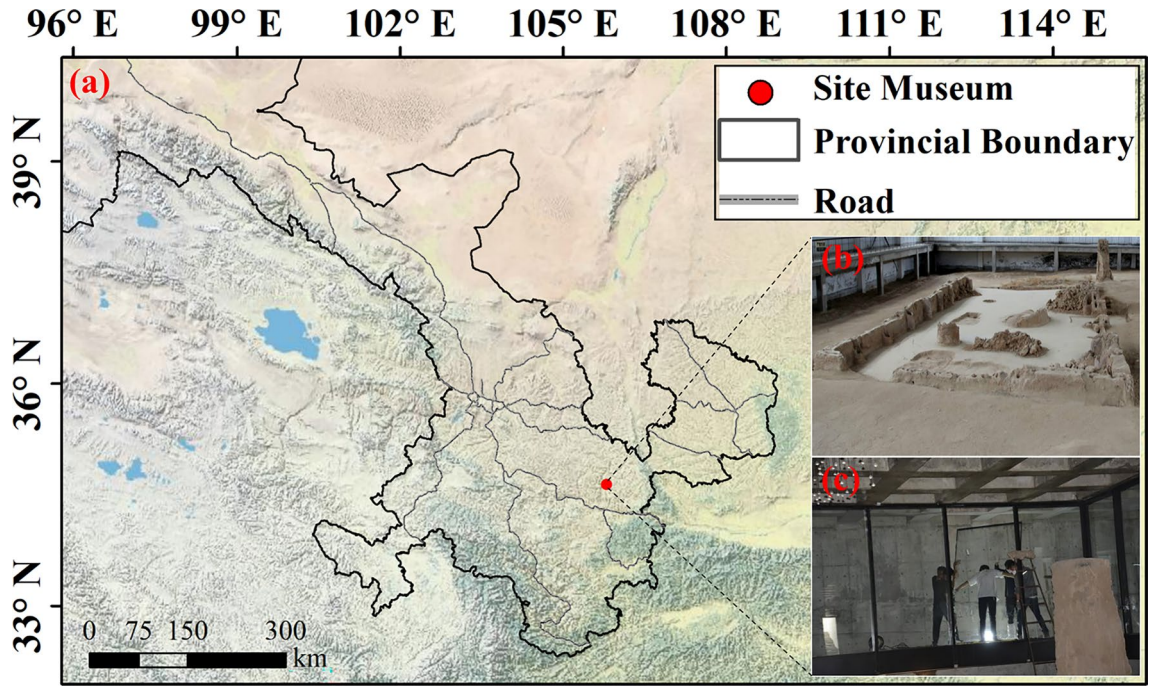

Fig. 1 Study area. **a** The location of the Dadiwan site; **b** Interior of the site; **c** Peripheral glass curtain walls

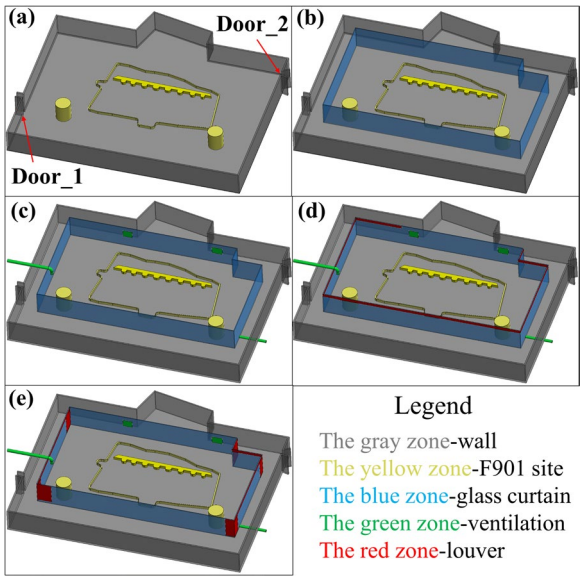

Fig. 2 Conceptual diagrams of site modifications at different protection stages. **a** Phase I; **b** Phase II; **c** Phase III; **d** Phase IV; **e** Phase V

Table 1 The information of measuring instrument

Item	Instrument type	Precision	Sampling interval
Temperature	HOBO MX2301	±0.2℃	10 min
Relative humidity	HOBO MX2301	±2.5%	10 min

installed to improve air circulation and reduce excessive humidity at the site. During phase IV (Fig. 2d), which took place from June 2019 to June 2020, the partial glass curtain walls were removed and replaced with louvered ventilation windows. During phase V (Fig. 2e), which took place from June 2020 to the present, additional optimization measures were undertaken, such as the substitution of five glass curtain walls with louvered ventilation windows, enhancement of duct fans power, and installation of three mesh doors at the major entrances.

Field monitoring

Environmental monitoring is an essential approach for safeguarding cultural heritage [28, 29]. Temperature and relative humidity are closely related to the occurrence and development of cultural heritage deterioration. Murals or earthen cultural relics are particularly concerned with the salt weathering caused by fluctuations in relative humidity, leading to phenomena such as efflorescence and alkali deterioration. Microbial disease focuses more on high relative humidity and water activity, which provide conditions favorable for microbial growth and activity. Therefore, the monitoring primarily concentrated on indoor and outdoor temperature and relative humidity. Specifics about the measuring instruments are provided in Table 1.

The monitoring points are situated in the following positions: the northwest corner, southwest corner, northeast corner, southeast corner, backfill region, center region, and corridor of the site. As seen in Fig. 3, all positions, with the exception of the corridor, are furnished with monitoring stations at three different elevations: 20 cm, 180 cm, and 300 cm.

Numerical simulation

General setup

Computational Fluid Dynamics (CFD) method simulates and evaluates the processes such as fluid flow and heat

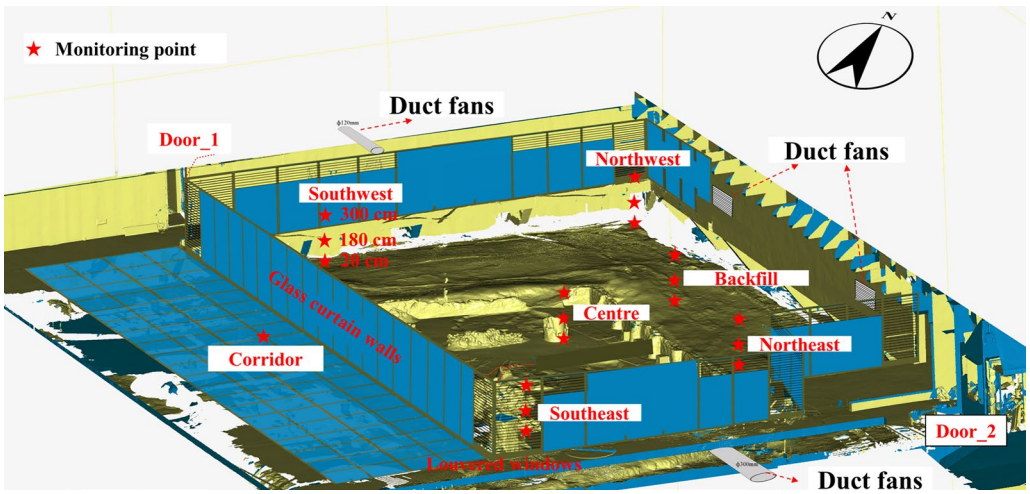

Fig. 3 Layout of monitoring points inside and outside the site

conduction. The simulation results provide the spatial distribution of fundamental physical parameters (such as velocity, pressure, temperature, etc.) at different points within the intricate flow domain. If we assume that the airflow is constant and not compressible, and has three dimensions, the equations that regulate continuity and momentum conservation may be represented as follows:

$$\frac{\partial \overline{u}_i}{\partial x_i} = 0 \tag{1}$$

$$\overline{u}_j \frac{\partial \overline{u}_i}{\partial x_j} = -\frac{1}{\rho}\frac{\partial \overline{p}}{\partial x_i} + \nu \frac{\partial^2 \overline{u}_i}{\partial X_j^2} - \frac{\partial}{\partial x_j}\left(\overline{u_i' u_j'}\right) + S_i \tag{2}$$

where $\overline{u}_i$ and x_i represents the average velocity component and direction, ρ is the density, t is time, $\overline{p}$ is the average pressure, and S_i is the source term.

In this study, we employed the professional CFD software Ansys Fluent and established the actual temperature, relative humidity, roughness, and other parameters corresponding to each boundary. Given that Eqs. (1) and (2) lack time-dependent terms, the simulation was conducted as a steady-state analysis. The SST *k-omega* turbulence model was used to calculate the distribution of the flow field. Subsequently, the species transport model was activated to simulate the coupled process of water vapor and air. This involved setting the initial boundary conditions, and halting the simulation once the residuals of all variables converged. To align with the five stages of the archaeological site renovation, five cases were set up for simulation, as shown in Table 2.

Model and mesh generation

Based on the design drawings of the site and field surveys, a three-dimensional building model is created in the modeling and meshing software ICEM. This model is based on the actual dimensions of the site and includes the internal spaces, walls, glass, louvers, entrances, exits, duct fans, and other overall structures related to airflow within the site. Spatial meshing is conducted as illustrated in Fig. 4a–d. The dimensions of the model are 50×33 m in the horizontal direction and 4.8 m in the vertical. The gray area in the image represents the wall, the yellow area represents the site, which is also the area for temperature and relative humidity monitoring. The blue area represents the glass curtain wall, and the light blue and red areas represent horizontal and vertical louvers. The mesh size is determined after a series of trials using the mesh-convergence index method. Therefore, the minimum mesh size is 0.2 m, and the total number of mesh is about 1.78×10^6.

Setting of boundary conditions

Based on on-site observations, we selected actual moments with significant differences of indoor and outdoor relative humidity in the numerical simulation process. Considering that air may blow into the site from either direction, the initial and boundary conditions for various cases in the computational domain are set as follows:

In scenario one, the air velocity at the door_1 is set to 0.5 $m\ s^{-1}$, with a relative humidity of 50% and a temperature of 25 °C. The roof is equipped with waterproof insulation, thus the impact of solar radiation on the walls and interior temperature is disregarded. The initial temperature of the roof and walls is set to 18°C, with no relative humidity specified. The ground, influenced by soil moisture, is treated as a source term, with initial temperature and relative humidity set to 18°C and 90%, respectively. The initial temperature and relative humidity within the interior space of the site were set to 18°C and 90%, respectively. The ventilation facilities are designated as outlet-vent boundaries, and the airflow rates were set to 250 $m^3\ h^{-1}$, 250 $m^3\ h^{-1}$, 900 $m^3\ h^{-1}$ in different cases, respectively. The louvers around the glass are simplified to porous media with a "porous-jump" boundaries, with a ventilation coefficient set at 80%. The door_2 is set to free outflow. The simulation begins with the initial outdoor air values remaining constant, and the analysis continues until the indoor temperature and relative humidity reach a stable state. Another actual moment with small differences in indoor and outdoor relative humidity is a relative humidity of 72% with a temperature of 7 °C in

Table 2 Setting of different simulation cases

Name	Stage	Protective measures
Case 1	I	/
Case 2	II	Glass curtain
Case 3	III	Glass curtain + ventilation facility + duct flow: 250 $m^3\ h^{-1}$
Case 4	IV	Glass curtain + ventilation facility + louver + duct flow: 250 $m^3\ h^{-1}$
Case 5	V	Glass curtain + ventilation facility + optimized louver + duct flow: 900 $m^3\ h^{-1}$

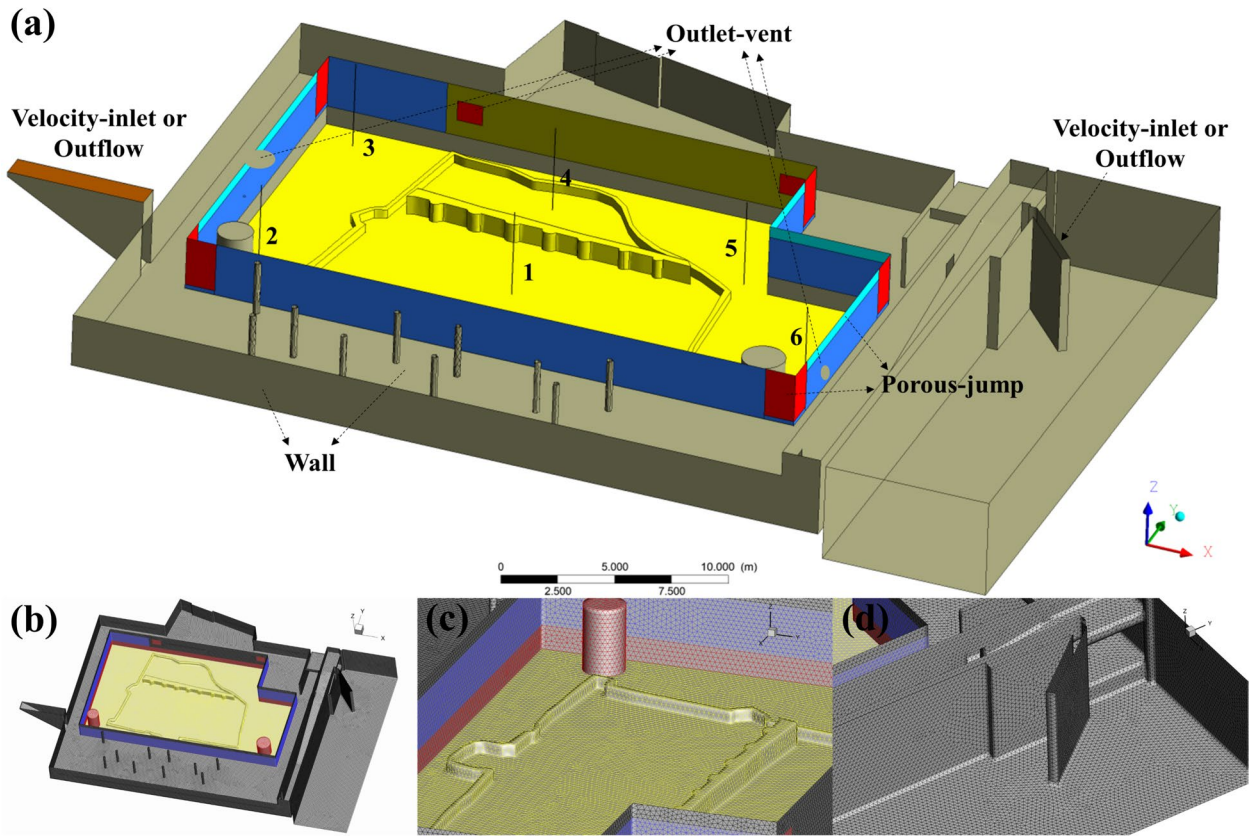

Fig. 4 Computing domain Settings. **a** Monitoring line settings; **b** Spatial meshing; **c** Internal meshing of the site; **d** Mesh details at door_2

inlet, while the internal relative humidity is 69% with a temperature of 2 °C. The other boundary conditions were essentially unchanged.

Scenario two considers an opposite wind direction and alters the initial conditions of the door_1 and door_2, while the initial values of the remaining boundaries remain unchanged.

In Fluent, the inlet conditions require the specification of the species mass fraction of water vapor rather than relative humidity. The relationship between relative humidity and the species mass fraction of water vapor is obtained from the following equations:

$$d = 0.622\frac{\varphi p_s}{p - \varphi p_s} \tag{3}$$

$$w = \frac{d}{1 + d} \tag{4}$$

where d represents specific humidity ($g\ kg^{-1}$), φ represents relative humidity (%), p represents air pressure (Pa), p_s represents saturated water vapor pressure corresponding to the dry-bulb temperature (Pa), and w represents the mass fraction of water vapor (%).

To compare the differences between different measures, six monitoring lines are established from the ground to the top of the site before numerical simulation. After the numerical simulation ends, the data on the monitoring lines can be directly obtained from the software for comparison with the measured data (Fig. 4a). The monitoring lines numbered 1 to 6 in the figure correspond respectively to the real-time monitoring points located at the center region, southwest corner, northwest corner, backfill region, northeast corner, and southeast corner (Corresponds to Fig. 3). This allows for a direct comparison of numerical differences between the cases.

Model verification

In order to enhance the credibility of the numerical simulation, a direct comparison was conducted between the simulation results and the real-time monitoring data. The analysis specifically focused on monitoring positions 1 to 6 (Figs. 5, 6). The relative humidity was measured to be about 70–72% at locations 20 cm, 180 cm, and 300 cm, and the simulated

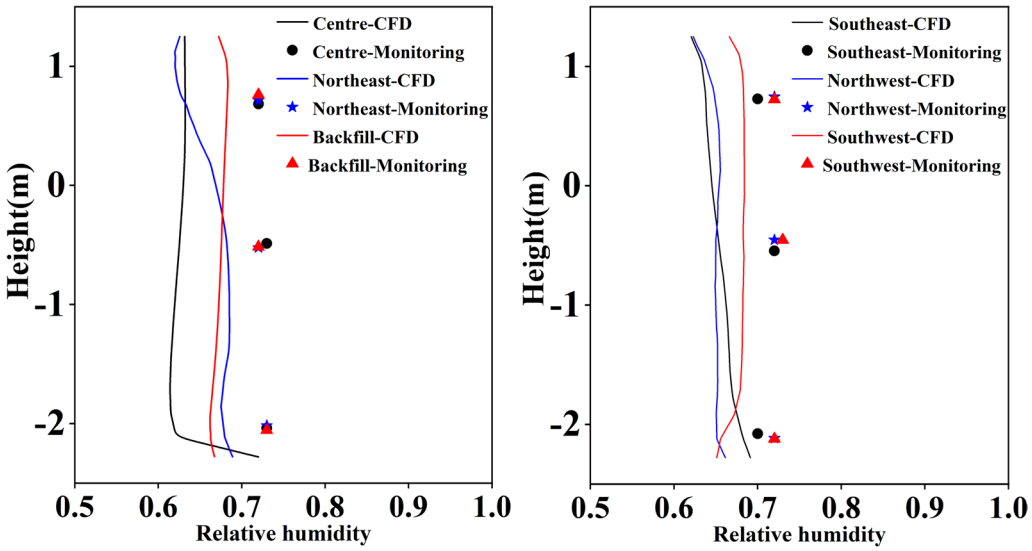

Fig. 5 Comparison of numerical simulation and measured results of relative humidity for monitoring lines 1 to 6

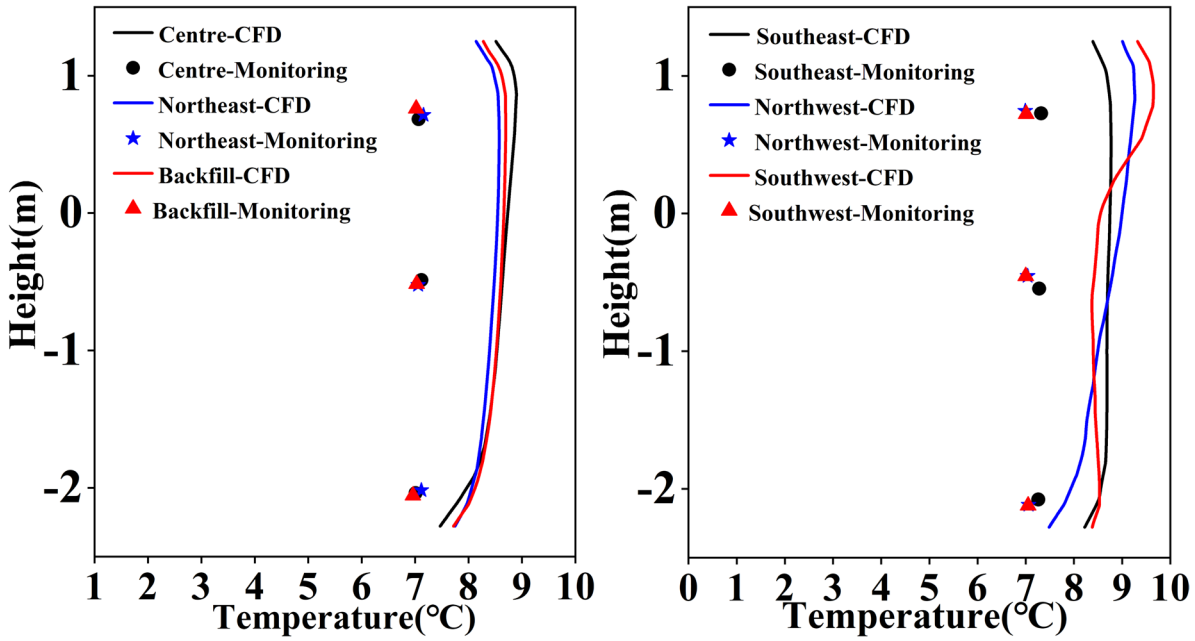

Fig. 6 Comparison of numerical simulation and measured results of temperature for monitoring lines 1 to 6

values mainly fell within the range of 62–70%. At the same location, the observed temperature range was 7.8–9.6 °C, while the simulated temperature range was 7.0–7.3 °C. We calculated the relative errors between measured and simulated results at different positions and heights. The results indicate that the relative errors of most simulated values compared to measured values of relative humidity and temperature are less than 15%.

Results

Analysis of measured relative humidity

Average monthly relative humidity

The center section of the site exhibited a similar trend to outdoor relative humidity variation, with higher levels observed during summer and lower levels during winter, as illustrated in Fig. 7. The relative humidity within and outside the site exhibited distinct variations under various protection measures:

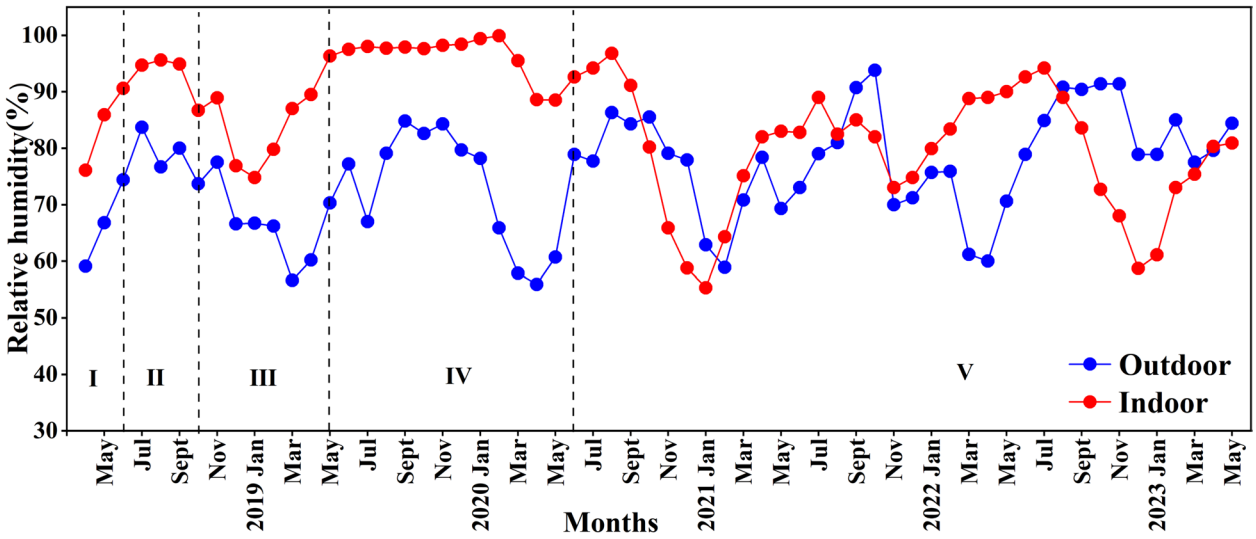

Fig. 7 The monthly average changes of relative humidity inside and outside the site from April 2018 to May 2023

Phase I (Before June 2018): Before the construction of the glass curtain wall, the interior relative humidity of the site fluctuated in accordance with the outside humidity. As a result of the lack of a glass curtain wall, there was a substantial flow of air between the interior and outdoor spaces, resulting in an average indoor relative humidity of around 84%. Phase II (June to October 2018): The indoor relative humidity gradually increased after the installation of the glass curtain walls and before the installation and opening of ventilation facilities. The interior average relative humidity significantly exceeded that of the external environment, with an average indoor relative humidity of up to 93%, even reaching saturation. Phase III (October 2018 to May 2019): The ventilation systems inside the facility were activated, resulting in a reduction in indoor relative humidity. The mean indoor relative humidity was around 85%.

Phase IV (May 2019 to June 2020): The indoor relative humidity steadily increased and, at one point, reached saturation. The monthly variation in relative humidity steadily decreased, reaching an indoor average of 98%. This time coincided with the primary period of the onset and dissemination of microbial diseases. In March 2020, the management office removed partial glass curtain walls located on the eastern and western sides of the property, therefore improving the circulation of air within. As a consequence, there was a drop in the indoor relative humidity, an increase in monthly variation, and an estimated 10% decline in the average indoor relative humidity.

Phase V (June 2020 to May 2023): The enhanced ventilation between interior and outdoor spaces resulted in a significant decrease in indoor relative humidity. The average relative humidity remained consistently around 70% during much of the year, with a reduction of around 18% compared to 2018 and 23% compared to 2019. The desired objective of enhancing the environment was successfully accomplished, thereby curbing the proliferation of microbiological infections inside the area.

It is noteworthy that Fig. 7 showed fluctuations in the indoor and outdoor relative humidity distribution from January to July 2022, with the relative humidity inside the site being higher than outside and the renovation measures did not appear to be effective. This was primarily due to the outbreak of COVID-19 pandemic in China at the time, which led to delays in opening the museum and activating ventilation systems. Consequently, the internal relative humidity increased as the climate warmed. After the ventilation systems were activated, monitoring data indicated that the relative humidity inside the site could be maintained at a stable level.

Relative humidity per 10 min

The real-time monitoring data of relative humidity at 10-min intervals provide a clearer reflection of the detailed changes in relative humidity inside and outside the site (Fig. 8). Throughout the monitoring period, outdoor relative humidity exhibited significant fluctuations, ranging from 5% to 100%, while indoor relative humidity fluctuated between 35% and 100%. During phase I without any protective measures, indoor relative humidity fluctuated greatly due to the influence of outdoor relative humidity. During phase II, the use of glass curtain walls prevented indoor relative humidity from fluctuating with external changes but maintained indoor relative humidity at above 90%. During phase III, the installation

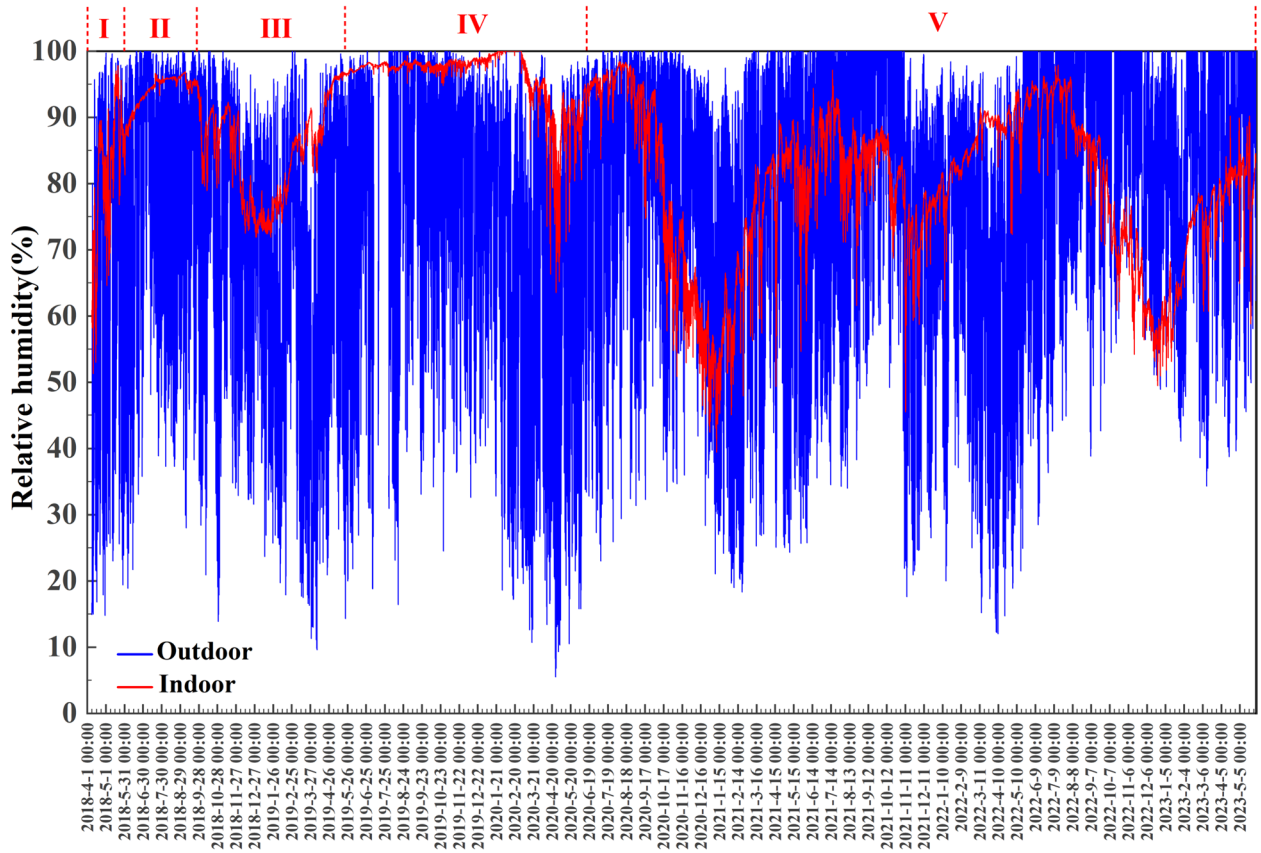

Fig. 8 The 10-min changes of relative humidity inside and outside the site from April 2018 to May 2023

of ventilation facilities reduced the fluctuation of indoor relative humidity from 70% to 90%, alleviating the high relative humidity environment within the site.

In the early stages of phase IV, indoor relative humidity approached saturation but later decreased. The saturation of indoor relative humidity may be because the site is an earthen relic, the high humidity environment in the early stages primarily occurred during the summer, where heat and moisture were generated from the ground, with high temperatures accelerating the dissipation of heat and moisture within the site. This process was significantly improved later as winter approached.

During phase V, improvements in internal ventilation and dehumidification conditions ensured that even with drastic fluctuations in outdoor relative humidity, indoor relative humidity remained between 35% and 90%, with an average relative humidity of around 70%, without reaching extreme states of saturation or supersaturation. During this stage, the relative humidity exhibited regular fluctuations with seasonal changes, demonstrating overall stability in fluctuations.

Simulated relative humidity distribution

Numerical simulation results provide comprehensive information on the flow field and the distribution of physical quantities at different locations. To avoid redundant presentation of results, we provide scenario one set of simulation results. The analysis of relative humidity at a 20 cm height above the ground indicated that, in the absence of protective measures, the internal relative humidity of the location was mostly impacted by external humidity. Locations near the entry and situated between the entrance and exit, where air circulation conditions were comparatively favorable, with a lower relative humidity level. The relative humidity near the entrance was approximately 40–50%, while at the entire exit, it was below 30%. Conversely, the overall humidity level in the entire space was higher, especially in the corridor area at the northwest corner, where the relative humidity exceeded 90% (Fig. 9a). Following the construction of the glass curtain walls (Fig. 9b), the site became more closely confined, resulting in limited air circulation. Due to the higher soil moisture within

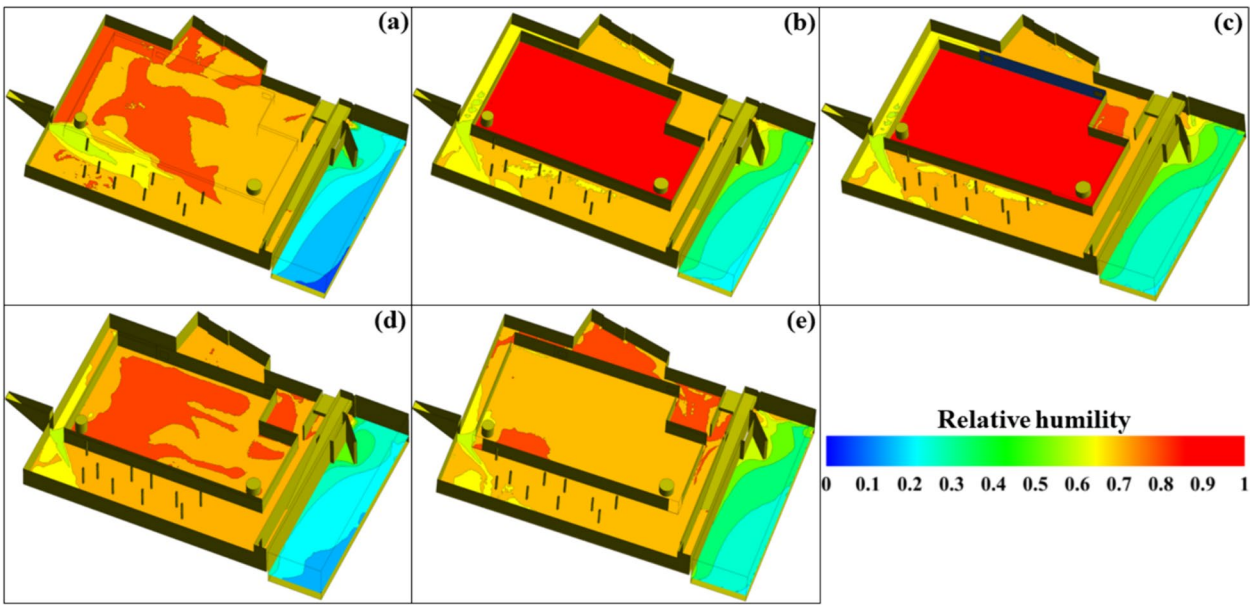

Fig. 9 Comparison of relative humidity distribution at 20 cm height above ground. **a** case 1; **b** case 2; **c** case 3; **d** case 4; **e** case 5

the site, the high-temperature environment caused the internal relative humidity to approach saturation, with the overall relative humidity within the entire space reaching nearly 100%. The airflow can only exit via the outside corridor of the glass curtain wall, resulting in a reduction in relative humidity in that area, maintaining the relative humidity in the corridor area at 60–70%. The implementation of these precautionary measures was unreasonable and significantly contributed to the development of microbiological infections. Upon the activation of the ventilation facilities (Fig. 9c), the decrease in internal humidity was not substantial owing to the low flow rate of the duct fans, suggesting inadequate ventilation efficiency.

By partly removing the glass curtain walls and replacing them with louvers (Fig. 9d), the blocking impact of the surrounding walls on the interior site was reduced. This led to a notable reduction in internal relative humidity compared to the previous stage. Nevertheless, in several regions, the relative humidity remained over 90%, therefore falling short of the rehabilitation criteria. By further optimizing the quantity and placement of louvers, and increasing the flow rate of duct fans (Fig. 9e), the internal ventilation system was able to effectively transfer water vapor to the corridor. The relative humidity in the corridor region exhibited a rise in comparison to the previous stage, reaching over 80%. However, the distribution of relative humidity in the majority of places within the site remained consistent and stable, generally maintaining around 70%. Thereby, the final renovation measures attained the anticipated objective of enhancement.

The relative humidity distribution at ground elevations of 180 cm and 300 cm inside the site is shown in Figs. 10 and 11. The heights displayed outcomes that were largely congruent with those seen at a distance of 20 cm from the ground. In the absence of any protective measures, the internal relative humidity of the site fluctuated in response to external circumstances by around 70–80% (Figs. 10a, 11a). Due to the obstruction of the surrounding glass curtain walls, the indoor relative humidity approached 100%, reaching a saturated state (Figs. 10b, 11b). When the ventilation facilities were activated, the airflow through the duct fan was low, resulting in only tiny regions of low humidity around the duct fan location. The relative humidity near the fan was in the range of 60% ~ 70% (Figs. 10c, 11c). By improving the placement and quantity of louvers and enhancing the capacity of the duct fans (Figs. 10d, e, 11d, e), these actions successfully ensured a steady and low-humidity environment across the whole site. Furthermore, owing to its substantial distance from the damp ground of the archaeological site, the relative humidity consistently remained below 70%.

The analysis results for scenario two are provided in supplementary material, as the distribution of relative humidity at different heights of the site is essentially consistent with scenario one when the boundary conditions of the inlet and outlet doors are swapped. During the first stage, when natural ventilation was employed, soil moisture evaporation caused the internal relative humidity to average around 80% (Figs. A1a, A2a, A3a). In the second stage, the use of glass curtain walls resulted in a saturated internal relative humidity of 100% (Figs. A1b,

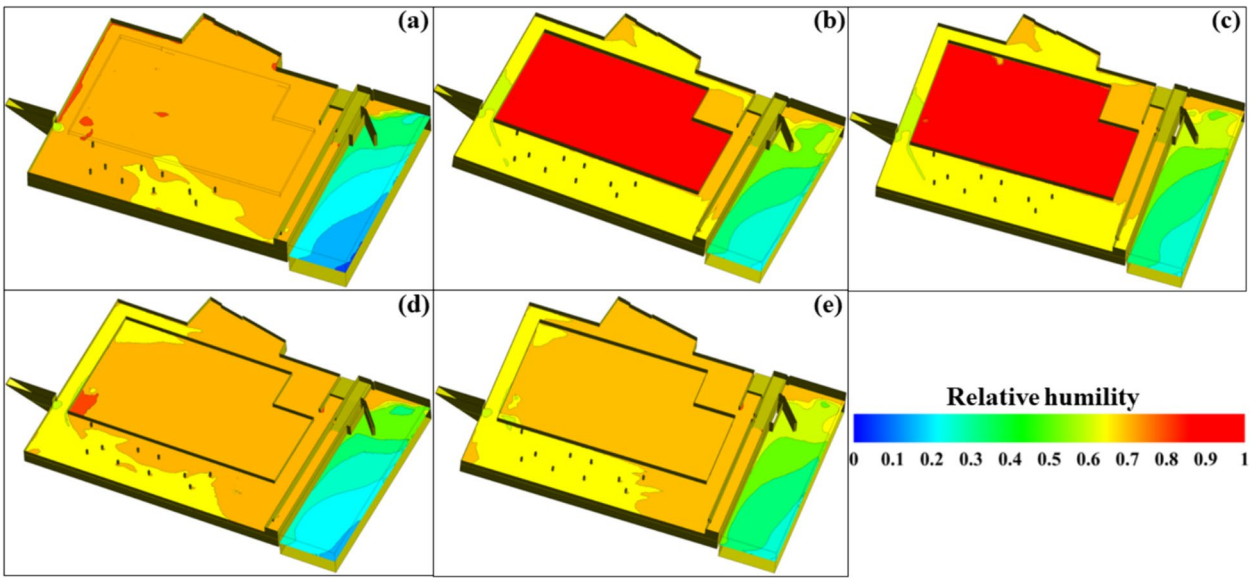

Fig. 10 Comparison of relative humidity distribution at 180 cm height above ground. **a** Case 1; **b** Case 2; **c** Case 3; **d** Case 4; **e** Case 5

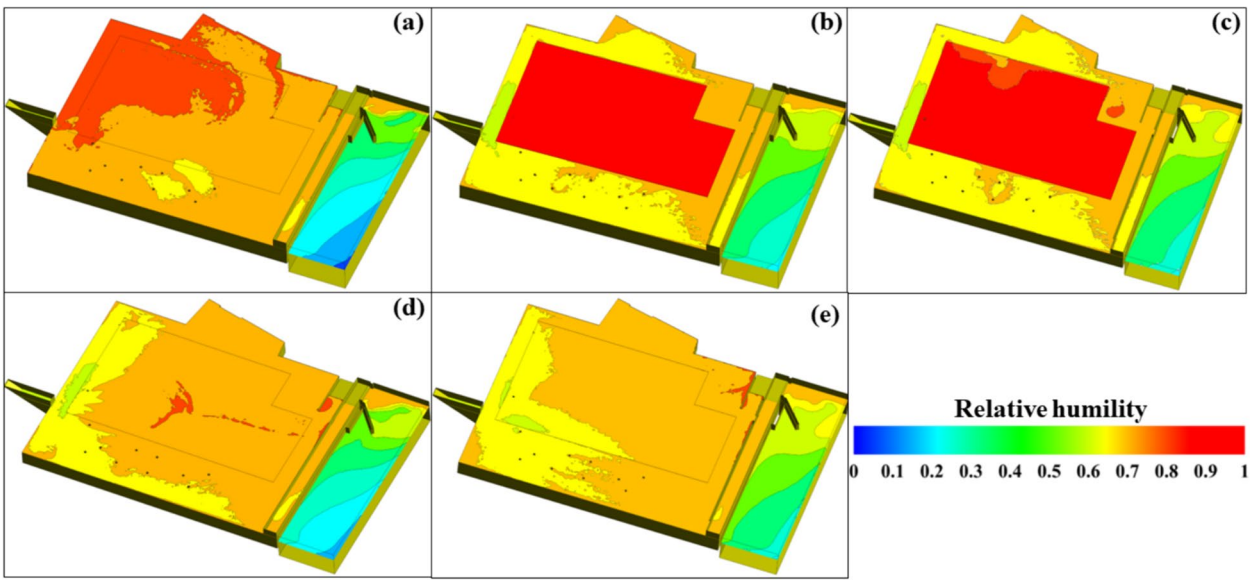

Fig. 11 Comparison of relative humidity distribution at 300 cm height above ground. **a** Case 1; **b** Case 2; **c** Case 3; **d** Case 4; **e** Case 5

A2b, A3b). In the third stage, with the introduction of low-flow ventilation systems, the relative humidity in certain areas decreased compared to the previous stage, with the northwestern corner exhibiting relative humidity levels between 60% and 70% (Figs. A1c, A2c, A3c). In the fourth stage, after replacing parts of the glass curtain walls with louvered windows, the relative humidity further decreased, with areas near the exhaust pipe showing levels below 70% (Figs. A1d, A2d, A3d). Finally, in the fifth stage, optimizing the number of louvered windows and increasing the exhaust flow maintained the internal relative humidity at 60% to 70% (Figs. A1e, A2e, A3e). This indicated that these optimization measures effectively reduced the relative humidity inside the site even under different boundary conditions.

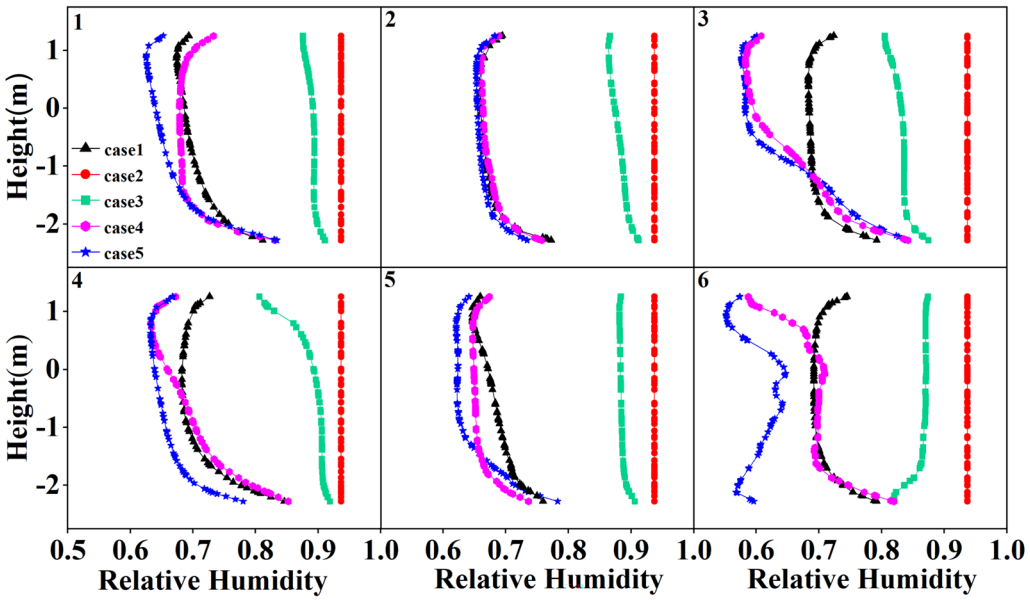

Fig. 12 The comparison of relative humidity at six monitoring line positions under different renovation measures

Monitoring line comparison

The comparison of monitoring line placements yielded a more accurate representation of the disparities in different protective measures. According to Fig. 12, the installation of the glass curtain walls resulted in a consistently high indoor relative humidity of 93% at every location and height. Upon activating the ventilation facilities, the relative humidity was reduced, however, it remained greater than the relative humidity of the external. The interior humidity at the site was dramatically reduced by augmenting the quantity of louvered ventilation windows and enhancing the flow rate of the duct fans. Consequently, the total relative humidity was consistently maintained at about 70%. This demonstrates that by optimizing the renovation measures, the ventilation and dehumidification facilities ultimately fulfilled the criteria for preserving cultural relics.

Nevertheless, the site's location in a depression resulted in elevated soil moisture levels. Additionally, the entry and exit were situated in the southwest and northeast

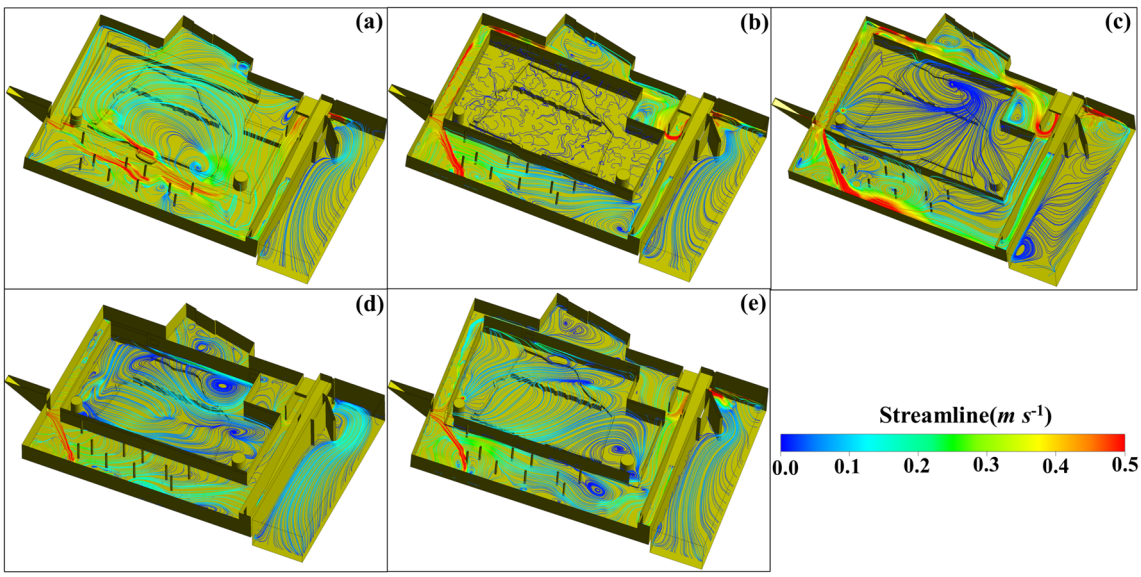

Fig. 13 Comparison of particle motion distribution. **a** Case 1; **b** Case 2; **c** Case 3; **d** Case 4; **e** Case 5

corners, posing challenges for air circulation, especially in the northwest corner. Despite implementing various measures such as exhaust systems, dehumidification, and louvered windows, a limited number of places nonetheless encountered a relative humidity as high as 84% (Fig. 12 (3) at the bottom). Hence, the positioning of duct fans should have considered the presence of corners and backflow areas.

Flow distributions analysis

The visual observation of relative humidity may be achieved by studying the trajectories movement and the influence of airflow and moisture movement. Figure 13 illustrated the flow analysis for scenario one. In the absence of the glass curtain walls, there is a dynamic circulation between the entry and exit, which effectively eliminates a portion of the air with greater humidity (Fig. 13a). However, during this phase, indoor relative humidity fluctuated with external changes, as high-humidity outdoor air was brought indoors through airflow circulation. In the absence of intervention measures, the relative humidity within the site underwent significant changes.

Upon the installation of the glass curtain walls (Fig. 13b), it effectively separated the interior site from the exterior air exchange. This method effectively maintains the stability of indoor environmental elements. The fully enclosed glass curtain wall can suppress the dependence of indoor humidity fluctuations on external weather fluctuations but has led to unintended consequences. The airflow was redirected towards the exterior corridor, diminishing its capacity to dissipate interior moisture. The inside airflow had little convection with the exterior environment, resulting in stagnant air and preventing the transportation of high-humidity air outside. The discontinuous streamline within the glass curtain wall in the diagram clearly reflects the stagnation of airflow within the site, significantly reducing the flow efficiency. As a result of this condition, the relative humidity in the site reached a level close to saturation, increasing the likelihood of microbiological outbreaks.

Upon activating the ventilation facilities (Fig. 13c), despite the low flow rate of the duct fans, observable airflow movement was still present in the vicinity of the fans. Compared to the stagnant airflow within the fully enclosed glass curtain wall, although the airflow velocity within the site is less than 0.1 m s^{-1} after opening the low-flow ventilation facilities, it generally maintains a slow internal airflow circulation. A certain amount of water vapor was released externally, leading to a decrease in the level of relative humidity.

By installing louvered windows and improving the flow of duct fans (Fig. 13d), the airflow can be enhanced to facilitate convection between the external air and the internal site through the louvered windows surrounding the glass. Ventilation facilities can effectively improve local airflow, but larger spatial layouts can only maintain a low-speed internal airflow circulation. Replacing the glass curtain wall with louvers can increase the exchange of external and internal airflow. The figure reflects that the airflow velocity in some areas of the site has increased to 0.15 m s^{-1}, but low-speed vortices with velocities less than 0.05 m s^{-1} still exist in areas like the northwest corner. This indicates that replacing louvers can enhance the airflow convection between indoors and outdoors, but their position and quantity still affect the spatial distribution of airflow.

By further optimizing the placement and number of louvered windows (Fig. 13e), the interior airflow was improved, resulting in a smoother flow compared to the previous stage. The flow velocity in most areas within the site exceeds 0.15 m s^{-1}. The airflow in the corner portions of the site was improved, resulting in a further reduction in the relative humidity of the air in these locations. The glass curtain wall effectively prevents the internal relative humidity of the site from changing with external conditions, while louvers and ventilation facilities ensure internal airflow circulation. Coordinating the relationship between enhancing air convection and preventing airflow exchange, contributed to the maintenance of a consistent and even low level of relative humidity over the whole area.

Figure A4 in the supplementary materials depicted the flow distribution for scenario two. The internal airflow was essentially consistent with scenario one when air goes into the site from a different door. The difference was that the internal airflow velocity was below 0.1 m s^{-1} in center areas, and ranged between 0.1 and 0.3 m s^{-1} in the corridor area. This reduction in speed was primarily due to the wall near door_2 obstructing the airflow.

Discussion

Cultural heritage preservation includes the processes of initial subterranean burial, non-sealed burial, and storage in museums after excavation. Within the enclosed subterranean burial chamber, the climatic conditions of the storage area for relics remain consistently steady, ensuring that the items maintain their original physical state. During the non-sealed burial phase, the equilibrium of environmental components, such as the initial temperature, relative humidity, and microbes, is disrupted by human activity or other reasons. During the post-excavation phase, relics are relocated from their original setting, and human intervention mostly regulates environmental conditions. Consequently, the notable decay of excavated artifacts is ascribed to the volatile outdoor weather

conditions and imbalanced soil-air conservation habitats [30].

The F901 site in Dadawan utilizes in-situ preservation techniques, which are part of the ongoing process of conserving cultural assets throughout the non-sealed burial stage. At first, the interior temperature and relative humidity at the location fluctuated in accordance with the external circumstances. Following the first renovation project, the installation of the glass curtain walls enclosure resulted in a consistent rise in interior temperature and relative humidity, with the relative humidity almost approaching saturation. According to the real-time on-site monitoring data, the average interior relative humidity reached a maximum of 93% at this stage, while the average outside relative humidity was 77.7%. The indoor relative humidity significantly exceeded that of the external environment. Soil moisture and wall moisture were the main factors affecting indoor relative humidity [31]. The subsequent activation of low-flow ventilation facilities had a negligible impact. Between May 2019 and June 2020, the indoor relative humidity steadily increased, exhibiting a consistent range of fluctuations. The monthly mean relative humidity varied between 88.5% and 100%, whilst the average outdoor relative humidity ranged from 55.9% to 84.8%. The presence of elevated temperature and humidity inside led to a significant proliferation of microorganisms, resulting in the continual occurrence of microbial infections that affected the relics. Therefore, dramatic changes in the thermal and humid environment will trigger the deterioration of historical artifacts [32]. This suggests that the initial rehabilitation attempt was ineffective, and instead, protective measure performed by humans resulted in the rapid deterioration of the cultural artifacts.

Implementing an optimized ventilation system has been empirically shown as an effective method for safeguarding cultural artifacts [33]. During the final phases of the restoration, specific precautions were taken depending on the site's peculiarities, natural environment, microbiological infections, and other factors. The steps implemented were converting the glass curtain walls into louvered ventilation windows, and enhancing the capacity of duct fans, to improve exhaust and dehumidification capacities. The numerical simulation results demonstrate that the final restoration measures greatly enhance the ventilation efficiency and dehumidification impact inside the site. They simultaneously ensure the consistency and steadiness of the air's temperature and moisture conditions inside the spatial region of the location, with an overall indoor relative humidity level of around 70%.

Referring to the Museum Environmental Preservation Standards—ASHRAE Handbook Class D standards, the recommended indoor relative humidity range is 25% to 75% throughout the year [34]. We have noted that Class D of the ASHRAE Handbook does not specify a temperature standard. The primary reasons we did not increase the temperature to lower the relative humidity are as follows: firstly, the preservation requirements of the site limit drastic temperature changes to avoid damage to artifacts. Secondly, using solar radiation to increase temperature introduces uncertainties and makes precise temperature control challenging. Therefore, we opted methods such as enhanced ventilation and dehumidification to control the relative humidity, taking these factors into full consideration in our study. Moisture is a key factor that can lead to deterioration [35]. The level of relative humidity in the air is closely linked to the formation of salt efflorescence-crystallization cycles such as efflorescence and microbial outbreaks on the surface of cultural relics. This is why relative humidity is a key concern in cultural heritage conservation. Therefore, relevant standards and recommended relative humidity control values in museum artifact preservation have significant reference value. Reference similar museums of environmental conservation [36]: The fluctuations in the hygrothermal environment can promote the deterioration of the Maijishan Grottoes, and in the summer, indoor ventilation and dehumidification should be increased [37]. The Jinsha earthen relic average indoor humidity for a general average year was $77.5 \pm 6.6\%$ [38]. The No.1 Pit of the Terracotta Army Museum maintains a relative humidity of 7% to 67%, which is suitable for the preservation of soil sites and painted terracotta figures [39, 40]. The Banpo Museum maintains a relative humidity of 53% to 70%, essentially meeting the requirements for soil sites and pottery preservation. Qianling Museum's outdoor environment for preserving the stone inscriptions on the Sima Dao has a relative humidity of 26% to 52%, but due to outdoor exposure, the stone inscriptions are susceptible to frost damage. On the other hand, the semi-closed Zhang Huai Crown Prince's Tomb has a relative humidity of 64% to 85%, often exceeding 90% in the summer, resulting in aging, peeling of murals, and microbial diseases. The Maoling Museum's protective measures include an outdoor shelter, and the moisture factors mainly vary with the environment, with a relative humidity range of 40% to 61%, which leads to frequent damage to stone inscriptions from summer exposure and winter frost. The Zhouyuan Museum has an average relative humidity of 60%, essentially meeting the preservation requirements for bronze artifacts. When the relative humidity in museums falls below 70%, it often satisfies the preservation requirements for soil sites, ceramics, paintings, bronze artifacts, and similar items. Semi-closed buildings are more effective than open-air or outdoor shelters in providing protection.

The previous anthropogenic alterations made to the Dadawan F901 site museum resulted in a persistent rise in internal temperature and humidity, leading to the occurrence of microbiological infections. Subsequently, an exhaust system was implemented and upgraded, protective systems were refined, and ventilation efficiency was increased. The concerted efforts made involve continuously improving and adjusting enclosure strategies, moving from glass curtain walls to louvered ventilation windows, and improving mechanical systems. These efforts ultimately contribute to the ongoing protection and preservation of the Dadiwan F901 site.

Nevertheless, continuous study is being conducted on the optimal preservation environment for cultural treasures. The challenge faced by archaeological museums is how to appropriately control the environment while ensuring the long-term preservation of cultural relics, all the while maintaining the overall view of the excavation site. The existing air thermal and moisture environment variables fulfill the standards for artifact preservation when evaluated using single atmospheric environmental indicators (e.g. relative humidity, temperature). However, it is essential to conduct systematic studies and implement effective management strategies to address concerns related to the aging of relics, weathering, and microbiological illnesses to achieve accurate preservation.

Conclusion

This paper assesses the efficiency of ventilation in five different stages of renovation at the Dadiwan F901 site museum. The evaluation is done through on-site real-time environmental monitoring and numerical simulation methods. The study compares the distribution of relative humidity and particle movement inside the site under various protective measures. The main conclusions based on the above analysis are as follows:

1. The fully enclosed glass curtain wall can suppress the dependence of indoor humidity fluctuations on external weather fluctuations but has led to unintended consequences. The original glass curtain walls and other obstructions hinder air circulation, exacerbating the increase in relative humidity near the site. This leads to the saturation of indoor air relative humidity, promoting the proliferation of microorganisms.
2. Louvered windows enhance the circulation of air inside the historical site, while duct fans and other methods can decrease humidity in partial areas or to a certain degree. Through the strategic optimization of the placement and number of louvered ventilation windows, the augmentation of duct fans' power, and the implementation of further measures, the indoor relative humidity is effectively maintained at around 70%, therefore satisfying the prerequisites for artifact preservation.

When implementing practical solutions, it is crucial to take into account the specific layout features of the location and carefully set up various ventilation techniques to properly regulate the equilibrium between interior and outdoor temperature and relative humidity. Moreover, it is essential to conduct systematic studies and implement effective management strategies to address concerns related to the deterioration of artifacts due to aging, weathering, and microbiological illnesses to ensure accurate preservation.

List of symbols

x_i The direction
ρ The density, $kg\ m^{-3}$
t The time, s
$\overline{p}$ The average pressure, Pa
S_i The source term
φ The relative humidity, %
d The specific humidity, $g\ kg^{-1}$
w The mass fraction of water vapor, %
p The pressure, Pa
$\overline{u}_i$ The average velocity component, $m\ s^{-1}$
P_s The saturated water vapor pressure corresponding to dry-bulb temperature, Pa

Supplementary Information

The online version contains supplementary material available at https://doi.org/10.1186/s40494-024-01415-x.

Additional file 1.

Author contributions

Benli Liu: Writing–review and editing, Writing–original draft, Methodology, Data curation, Funding acquisition. Chenchen He: Writing–original draft, Software. Guobin Zhang: Methodology, Supervision, Investigation. Ruihong Xu: Investigation. Hongtao Zhan: Data curation. Fasi Wu: Data curation. Dongpeng He: Data curation.

Funding

This work was supported by the Research Project on Scientific and Technological Conservation of Cultural Relics in Gansu Province (GSWW202227), and the Excellent Member of Youth Innovation Promotion Association CAS (No. Y202085).

Data availability

No datasets were generated or analysed during the current study.

Declarations

Ethics approval and consent to participate

This research did not involve any human or animal experiments or other ethical considerations. All data and information were obtained through lawful research methods and adhered to relevant laws, regulations, and ethical guidelines during the research process.

Competing interests

The authors declare no competing interests.

Author details
[1]Key Laboratory of Ecological Safety and Sustainable Development in Arid Lands/Research Station of Gobi Desert Ecology and Environment in Dunhuang, Northwest Institute of Eco-Environment and Resources, Chinese Academy of Sciences, Lanzhou 730000, China. [2]University of Chinese Academy of Sciences, Beijing 100049, China. [3]The Conservation Institute of Dunhuang Academy, Dunhuang 736200, China.

Received: 23 April 2024 Accepted: 8 August 2024
Published online: 21 August 2024

References

1. Liu C. Discussion on the great historical contributions of Dadiwan ruins (**in Chinese**). J Hotan Teach Coll. 2006;3:206–7.
2. Liu L, Chen X. The archaeology of China: from the late paleolithic to the early bronze age. Oxford City: Cambridge University Press; 2012.
3. Li Z, Zhao L, Li L. Light weight concrete of Yangshao period of China: the earliest concrete in the world. Sci China Technol Sci. 2012;55(3):629–39.
4. Liu L. Communal drinking rituals and social formations in the Yellow River valley of Neolithic China. J Anthropol Archaeol. 2021;63:101310.
5. Li Z, Zhao L, Li L, Wang J. Research on the modification of two traditional building materials in ancient China. Herit Sci. 2013;1(1):2–11.
6. Liu L, Chen J, Wang J, Zhao Y, Chen X. Archaeological evidence for initial migration of Neolithic Proto Sino-Tibetan speakers from Yellow River valley to Tibetan Plateau. Proc Natl Acad Sci. 2022;119(51): e2212006119.
7. Wu W, Zheng H, Hou M, Ge Q. The 5.5 cal ka BP climate event, population growth, circumscription and the emergence of the earliest complex societies in China. Sci China Earth Sci. 2017;61(2):134–48.
8. Luo X, Huang X, Feng Z, Li J, Gu Z. Influence of air inlet/outlet arrangement of displacement ventilation on local environment control for unearthed relics within site museum. Energy Build. 2021;246:111116.
9. Jiang G, Guo F, Polk JS. Salt transport and weathering processes in a sandstone cultural relic, North China. Carbonates Evaporites. 2015;30:69–76.
10. Liu H, Chen Y. Spatial and temporal distribution characteristics of cultural relics protection units and disaster risk analysis in Beijing. ISPRS Ann Photogramm Remote Sens Spat Inform Sci. 2022;X-3/W1-2022:115–24.
11. Sawada M, Mimura M. Geotechnical approaches for preservation of openly exhibited Geo-relics damaged by rainfall infiltration. Soils Found. 2022;62(1): 101097.
12. Luo X, Gu Z, Yu C. Desiccation cracking of earthen sites in archaeology museum—a viewpoint of chemical potential difference of water content. Indoor Built Environ. 2015;24(2):147–52.
13. Franco-Castillo I, Hierro L, de la Fuente JM, Seral-Ascaso A, Mitchell SG. Perspectives for antimicrobial nanomaterials in cultural heritage conservation. Chem. 2021;7(3):629–69.
14. Feng Z, Luo X, Wang J, Cao SJ. Energy-efficient preservation environment control for enclosed exhibition hall of earthen relics. Energy Build. 2022;256: 111713.
15. Cao LNY, Cao J, Lee S, Zhang Y, Tie X. Numerical simulation of the micro environment in the Han Yang Mausoleum Museum. Aerosol Air Qual Res. 2012;12(4):544–52.
16. Xia Y, Fu F, Wang J, Yu CW, Gu Z. Salt enrichment and its deterioration in earthen sites in emperor Qin's Mausoleum Site Museum, China. Indoor Built Environ. 2023;32:1862.
17. Bi W, Yan Z, Zhang Z, Yao S, Zhang J, Wang X. Modeling and numerical simulation of heat and mass transfer in the cave wall of the Mogao Grottoes in China. Build Environ. 2021;201: 108003.
18. Ferdyn-Grygierek J, Grygierek K. Proposed strategies for improving poor hygrothermal conditions in museum exhibition rooms and their impact on energy demand. Energies. 2019;12(4):620.
19. Schito E, Conti P, Urbanucci L, Testi D. Multi-objective optimization of HVAC control in museum environment for artwork preservation, visitors' thermal comfort and energy efficiency. Build Environ. 2020;180: 107018.
20. Ferdyn-Grygierek J, Grygierek K. HVAC control methods for drastically improved hygrothermal museum microclimates in warm season. Build Environ. 2019;149:90–9.
21. Luo X, Gu Z, Yu C, Ma T, Kase K. Efficacy of an air curtain system for local pit environmental control for relic preservation in archaeology museums. Indoor Built Environ. 2016;25(1):29–40.
22. Bichlmair S, Raffler S, Kilian R. The temperierung heating systems as a retrofitting tool for the preventive conservation of historic museums buildings and exhibits. Energy Build. 2015;95:80–5.
23. Luo X, Gu Z, Tian W, Xia Y, Ma T. Experimental study of a local ventilation strategy to protect semi-exposed relics in a site museum. Energy Build. 2018;159:558–71.
24. Luo X, Lei S, Tian W, Gu Z. Evaluation of air curtain system orientated to local environmental control of archaeological museum: a case study for the stone armor pit of Emperor Qin's Mausoleum Museum. Sustain Cities Soc. 2020;57: 102121.
25. Perino M. Air tightness and RH control in museum showcases: concepts and testing procedures. J Cult Herit. 2018;34:277–90.
26. Chiantore O, Poli T. Indoor air quality in museum display cases: volatile emissions, materials contributions, impacts. Atmosphere. 2021;12(3):364.
27. Guo Q. The formation and early development of architecture in Northern China. Constr Hist. 2001;17:3–16.
28. Liu Y, Tang Y, Jing L, Chen F, Wang P. Remote sensing-based dynamic monitoring of immovable cultural relics, from environmental factors to the protected cultural Site: a case study of the Shunji Bridge. Sustainability. 2021;13(11):6042.
29. Centenaro S, Franceschin G, Cattaruzza E, Traviglia A. Consolidation and coating treatments for glass in the cultural heritage field: a review. J Cult Herit. 2023;64:132–43.
30. Luo X, Gu Z, Li T, Meng X, Ma T, Yu C. Environmental control strategies for the in situ preservation of unearthed relics in archaeology museums. J Cult Herit. 2015;16(6):790–7.
31. Liu F, Zhang X, Zeng J, Li Y, Wang G. The numerical study on indoor heat and moisture transfer characteristics of an ancient palace building in Beijing. Processes. 2023;11(7):1900.
32. Xiong J, Li A, Liu C, Dong J, Yang B, Cao J, Ren T. Probing the historic thermal and humid environment in a 2000-year-old ancient underground tomb and enlightenment for cultural heritage protection and preventive conservation. Energy Build. 2021;251: 111388.
33. Gu Z, Luo X, Meng X, Wang Z, Ma T, Yu C, Rong B, Li K, Li W, Tan Y. Primitive environment control for preservation of pit relics in archeology museums of China. Environ Sci Technol. 2013;47(3):1504–9.
34. Kramer R, Schellen H, van Schijndel J. Energy impact of ASHRAE's museum climate classes: a simulation study on four museums with different quality of envelopes. Energy Proc. 2015;78:1317–22.
35. Liu B, Peng W, Li H, Qu J. Increase of moisture content in Mogao Grottoes from artificial sources based on numerical simulations. J Cult Herit. 2020;45:135–41.
36. Ma T, Ma H. Research on the conservation environment of cultural relics in Shaanxi site and tomb museums. Shaanxi Environ. 2003;10(5):10–3 (**in Chinese**).
37. Yao S, Yan Z, Ma Q, Xu B, Zhang Z, Bi W, Zhang J. Analysis of the annual hygrothermal environment in the Maijishan Grottoes by field measurements and numerical simulations. Build Environ. 2022;221: 109229.
38. Yang S, Wu L, Wu B, Zhang Y, Wang H, Tan X. Diversity and structure of soil microbiota of the Jinsha earthen relic. PLoS ONE. 2020;15(7):1–18.
39. Cao J, Rong B, Lee S, Chow J, Ho K, Liu S, Zhu C. Composition of indoor aerosols at Emperor Qin's Terra-cotta Museum, Xi'an China, during summer, 2004. China Particuol. 2005;3:170–5.
40. Dang Y, Luo X, Chang B, Huang X. Local attachment ventilation system for the unearthed relic preservation area within site museum. Sustain Cities Soc. 2022;77: 103537.

Publisher's Note